

RELIABILITY SCALING LAWS FOR QUANTIZED LARGE LANGUAGE MODELS

Anonymous authors

Paper under double-blind review

ABSTRACT

Quantization is a powerful strategy to build capable and resource-efficient large language models (LLMs) by reducing the bitwidth of the parameters. While quantized LLMs achieve state-of-the-art performance on unperturbed inputs using standard predictive metrics, their performance on perturbed inputs, measured using subsidiary reliability metrics, remains underexplored, despite its importance for safe and reliable deployment. To address this gap, we conduct a comprehensive reliability evaluation of quantized LLMs consisting of three key components: **(1) Uncertainty:** We assess the trustworthiness of LLMs quantized to 2, 3, 4, and 8 bits using six different quantization methods, employing established uncertainty metrics operating at both token and sequence levels. **(2) Robustness:** We design character-level and word-level input perturbations to evaluate the reliability of quantized models under semantically-preserving variations in the inputs that commonly arise in real-world applications. **(3) Reliability scaling trends:** We investigate how the reliability scales with the total number of model bits. Interestingly, our study reveals that while the performance scales monotonically with the total number of bits, the reliability scalings show nonlinear trends. Specifically, a reliability peak occurs for 4-bit quantized models, indicating that quantizing moderately sized base models offers the best reliability-efficiency trade-off. Additionally, our empirical findings reveal that quantization can enhance the robustness of LLMs to natural input perturbations.

1 INTRODUCTION

Large language models (LLMs) (Touvron et al., 2023; Team et al., 2024; Wei et al., 2022) have reshaped the field of Natural Language Processing (NLP) with their remarkable performance across a range of complex benchmarks. Recent advances in LLMs are based on the principle that model performance improves predictably with increased model size and training data, following well-characterized scaling laws (Kaplan et al., 2020). However, their large size and high computational needs pose significant challenges for practical use, especially in resource-limited settings. This has spurred interest in model compression to reduce inference latency and memory requirements, including quantization (Dettmers et al., 2022; Lin et al., 2024a; Frantar et al., 2022), pruning (Sun et al., 2023; Frantar & Alistarh, 2023), and knowledge distillation (Gu et al., 2023; Liang et al., 2023).

Despite rapid progress in LLM quantization, their evaluation has predominantly focused on benign task performance, emphasizing that compressed models should retain the accuracy of the base model on downstream tasks (Lin et al., 2024a; Frantar et al., 2022; Sun et al., 2023; Frantar et al., 2025). While useful, these evaluations ignore critical reliability aspects, notably uncertainty and robustness, which are essential for a safe and trustworthy deployment. On the one hand, uncertainty quantification (Kadavath et al., 2022) and calibration (Krishnan et al., 2024) have gained significant traction to assess the trustworthiness of responses generated by LLMs. However, the impact of model quantization on these critical dimensions remains underexplored. On the other hand, quantized models deployed in practice may encounter minor input noise, such as typos or grammatical errors, while the semantics of the original sentence are preserved (Moradi & Samwald, 2021). Yet, commonly used benchmarks (Joshi et al., 2017; Reddy et al., 2019) for evaluating the capabilities of quantized models fail to capture such perturbations, limiting our understanding of model robustness in real-world applications.

054
055
056
057
058
059
060
061
062
063
064
065
066
067
068
069
070
071
072
073
074
075
076
077
078
079
080
081
082
083
084
085
086
087
088
089
090
091
092
093
094
095
096
097
098
099
100
101
102
103
104
105
106
107

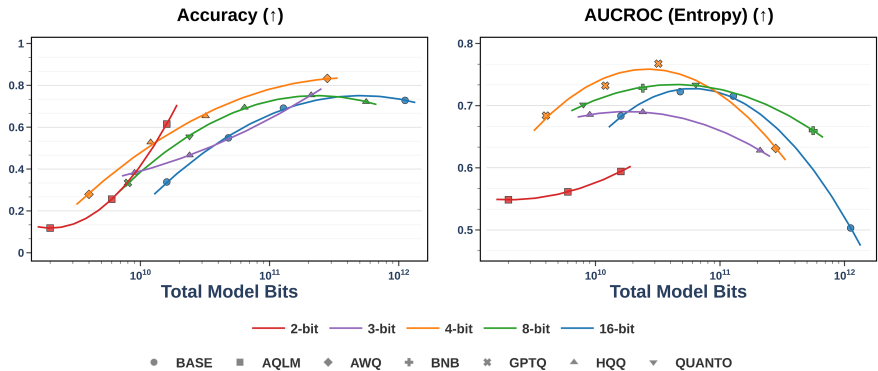


Figure 1: Bit-level scaling trends of the accuracy and AUCROC(Entropy) on TriviaQA (Joshi et al., 2017). We use four base models (blue): LLaMA-3.2-1B, LLaMa-3.2-3B, LLaMa-3-8B, and LLaMa-3-70B, and their corresponding quantized variants using six quantization methods and different bitwidths. We report accuracy for the downstream task performance and AUCROC (Entropy) for reliability evaluation.

To address these gaps, we conduct a comprehensive evaluation of quantized LLMs across multiple **reliability** dimensions, including *uncertainty*, and *robustness* to semantically-preserving input perturbations. To better understand how many bits should be used to improve the reliability-efficiency trade-off, we leverage **bit-level scaling laws**, which reveal underlying trends that extend beyond individual data points. Consider two models: One model trained from scratch with 4 billion parameters at 16-bit precision, and another model with 16 billion parameters quantized to 4-bit precision. While both have the same total number of bits, their behavior can differ significantly (Dettmers & Zettlemoyer, 2023). Prior work (Xu et al., 2024b; Dutta et al., 2024; Lin et al., 2024a; Dettmers & Zettlemoyer, 2023) mainly focus on assessing the effectiveness of the quantization methods by solely relying on the downstream task performance. In particular, Dettmers & Zettlemoyer (2023) explore bit-level scaling trends for standard task performance on different benchmarks, showing that accuracy typically improves with the total number of bits. However, we find that higher accuracy does not necessarily correspond to higher reliability. As shown in Fig. 1, accuracy scales monotonically with the total number of model bits. In contrast, reliability follows a non-monotonic trend: reliability peaks for moderately-sized models quantized to 4 bits, suggesting that an optimal trade-off can be achieved without resorting to either high-precision quantization or the largest model.

We highlight our main contributions in the following:

- We implement 15 character-level and word-level natural input perturbations, and study how quantization affects the robustness to semantically-preserving input noise.
- We study the bit-level scaling trends of post-training quantization methods to determine the precision that maximizes robustness given a specific budget of total model bits.
- We conduct the first comprehensive reliability evaluation of six state-of-the-art quantization techniques, on both *unperturbed* and *perturbed* input prompts. We examine which quantization methods improve the reliability scalings for 2 to 8-bit precision at scales of 1B to 70B parameters across LLaMA, OPT, and Qwen model families. Our key findings are: (i) Base and quantized models are sensitive to different character-level and word-level input perturbations. Our empirical results demonstrate that quantization not only enhances efficiency but also improves the robustness of LLMs to semantically-preserving input perturbations. (ii) Zero-shot performance scaling trends exhibit a different behavior than the reliability scaling trends. (iii) 4-bit precision offers the best reliability-efficiency trade-off across different tasks, model families, and quantization methods.

2 RELATED WORK

Scaling Laws for LLMs This work builds on established scaling laws that characterize how the training budget affects the performance of language models (Kaplan et al., 2020; Hernandez et al., 2021; Sorscher et al., 2022; Kumar et al., 2024). Kaplan et al. (2020) demonstrate that the model loss follows a power law with the number of model parameters and tokens. Building on this, Hoffmann

et al. (2022) argue that both model size and the number of training tokens should be scaled equally to achieve optimal compute training. Other works have shifted focus to the test-time budget, examining how quantization can impact the performance (Dettmers & Zettlemoyer, 2023; Kumar et al., 2024; Frantar et al., 2025). In this work, our goal is to understand the impact of the compression budget, defined as the total number of model bits, on downstream performance. Closest to our work are the bit-level scaling laws for zero-shot performance of quantized LLMs proposed in Dettmers & Zettlemoyer (2023), where the goal is to determine the precision that maximizes the accuracy. However, Dettmers & Zettlemoyer (2023) solely focus on scaling trends of downstream task performance, and do not account for critical reliability dimensions necessary for safe deployment.

Reliability Evaluation of LLMs With the increasing interest in LLMs, understanding uncertainty and calibration is crucial. Various uncertainty quantification methods have emerged to determine the trustworthiness of the generated responses by LLMs (Kuhn et al., 2023; Ye et al., 2024). Kuhn et al. (2023) introduce semantic entropy, which considers linguistic invariants arising from shared meanings. Malinin & Gales (2020) introduce predictive entropy, which quantifies the uncertainty of auto-regressive models based on their own outputs. Recently, Ye et al. (2024) employed conformal prediction to quantify the uncertainty of LLMs in NLP tasks, including question answering and reading comprehension. Calibrating the uncertainty estimates is essential to evaluating the reliability of LLMs. A well-calibrated model correlates low uncertainty with accurate responses and high uncertainty with likely incorrect responses. This is typically evaluated using the Expected Calibration Error (ECE) (Jiang et al., 2021) and the Brier Score (Brier, 1950). In generative tasks, defining calibration is often challenging (Kapoor et al., 2024), especially for variable-length response sequences.

While several studies have explored different reliability dimensions for LLMs, these aspects remain underexplored for quantized models. Most prior works on model compression, such as Lin et al. (2024a); Frantar et al. (2022); Frantar & Alistarh (2023); Team (2023); Ashkboos et al. (2024), primarily evaluate the effectiveness of compression methods through standard performance metrics, including perplexity and accuracy on various benchmarks. However, these benchmarks fail to capture critical aspects of model reliability. Recently, Hong et al. (2024) present a comprehensive evaluation of compressed LLMs across various trustworthiness dimensions including stereotype, toxicity, privacy, fairness, ethics, adversarial robustness, and out-of-distribution robustness. Their primary question of interest is how to construct trustworthy 7B models, either by pre-training from scratch or by compressing a larger pre-trained 13B model. (Hong et al., 2024) reveal that quantization offers a more favorable trade-off between efficiency and trustworthiness than pruning. Li et al. (2024) evaluate quantized models beyond trustworthiness dimensions, covering basic NLP tasks, long-context understanding, and emergent abilities, while Chen et al. (2025a) offer a safety evaluation of quantized LLMs. Both trustworthiness and safety evaluations provided in prior work are closely related to our study, intending to enable trustworthy deployment of quantized LLMs. However, we focus on studying the underlying bit-level scaling trends, providing insights beyond individual data points, and enabling direct comparisons across multiple model scales and bitwidths. Beyond safe deployment considerations, Dong et al. (2025) exploit quantization as a novel threat model to activate safety misalignment that is dormant in the full-precision counterparts.

3 RELIABILITY EVALUATION FRAMEWORK

Consider a pre-trained autoregressive language model $P_\theta(\mathbf{y} \mid \mathbf{x})$ parameterized by θ , where \mathbf{x} is an input prompt, and \mathbf{y} is the generated sequence. We adapt this model to downstream conditional text generation tasks, such as question answering. Each task is represented by a dataset of context-target pairs, $\mathcal{D} = \{(\mathbf{x}_i, \mathbf{y}_i^*)\}_{i=1}^N$, where both \mathbf{x}_i and \mathbf{y}_i^* are sequences of tokens. Given an input prompt \mathbf{x} , the model generates answer tokens sequentially as follows:

$$P_\theta(\mathbf{y} \mid \mathbf{x}) = \prod_{t=1}^T P_\theta(\mathbf{y}_t \mid \mathbf{y}_1, \dots, \mathbf{y}_{t-1}, \mathbf{x}), \quad (1)$$

where $\mathbf{y} = (\mathbf{y}_1, \dots, \mathbf{y}_T)$ is the final generated sequence consisting of T tokens. We denote the model’s predicted token distribution by $P_\theta(\mathbf{y} \mid \mathbf{y}_1, \dots, \mathbf{y}_{t-1}, \mathbf{x})$, where $\mathbf{y} \in \mathbb{R}^{|\mathcal{V}|}$, and \mathcal{V} is the vocabulary. At each decoding step t , the model samples a token $\mathbf{y}_t \sim P_\theta(\cdot \mid \mathbf{y}_{1:t-1}, \mathbf{x})$.

162
163
164
165
166
167
168
169
170
171
172
173
174
175
176
177
178
179
180
181
182
183
184
185
186
187
188
189
190
191
192
193
194
195
196
197
198
199
200
201
202
203
204
205
206
207
208
209
210
211
212
213
214
215

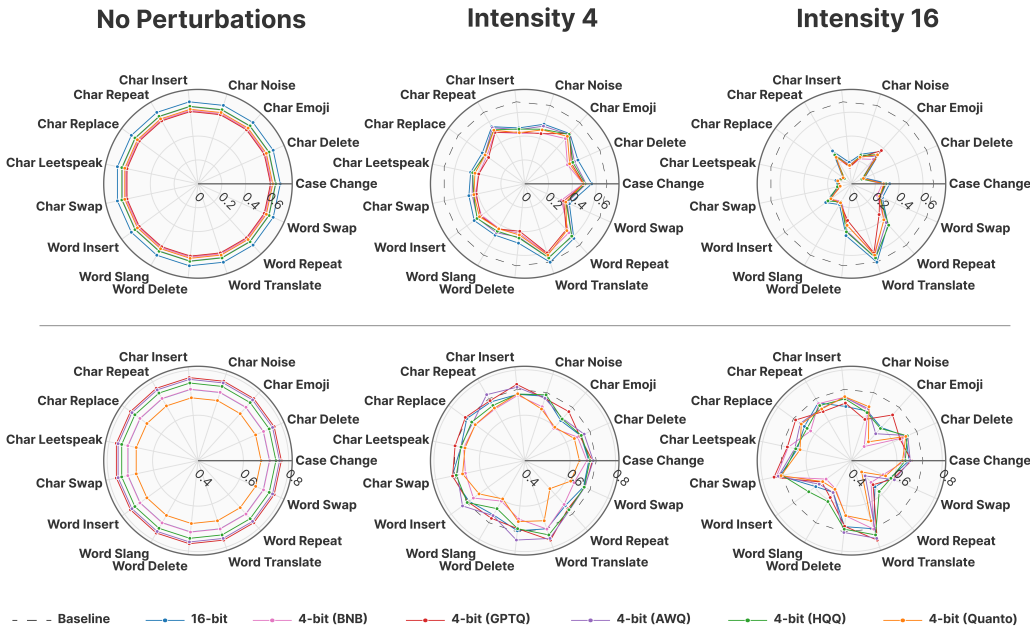


Figure 3: Radar plots of the accuracy (**Top**) and AUCROC (Entropy) (**bottom**) across all 15 character-level and word-level perturbations for two intensities. We evaluate the base LLaMa-3-8B model and five 4-bit quantization methods. Quantized models can provide more reliable uncertainty estimates under natural perturbations compared to their base counterparts, while maintaining a close performance.

To study the bit-level scaling, we consider quantization, which is a widely used compression technique that reduces the number of bits in the parameters of a model with minimal loss in inference performance (Dettmers et al., 2022; Lin et al., 2024a; Frantar et al., 2022; Team, 2023; Badri & Shaji, 2023).

3.1 RELIABILITY EVALUATION

In this paper, our goal is to evaluate various aspects of *reliability* for quantized LLMs in a question answering setting. Given an input prompt \mathbf{x} , $P_\theta(\mathbf{y} | \mathbf{x})$ spans a probability distribution of all possible output sequences. Although we are generally interested in the output distribution $P_\theta(\mathbf{y} | \mathbf{x})$, in practice, we cannot directly access this distribution since the number of possible output sequences $|\mathcal{V}|^T$ is large. Therefore, we first define our reliability metrics at the *token-level*, as we have direct access to the token distributions $P_\theta(\mathbf{y} | \mathbf{y}_{1:t-1}, \mathbf{x})$ at every step t , and aggregate these measures to obtain *sequence-level* metrics. Let M_t denote a token-level metric at step t , the sequence-level metric is computed as the average across all time steps:

$$M_{\text{seq}} = \frac{1}{T} \sum_{t=1}^T M_t. \tag{2}$$

Relying on a single generated sequence \mathbf{y} given an input prompt \mathbf{x} can lead to an incomplete assessment in a natural language generation (NLG) setting. To provide a more robust and representative estimate of the model’s reliability, we sample multiple sequences per input prompt and report averaged results across these samples. In the following, we outline the different reliability metrics measured on the token level. To measure the model’s uncertainty in the predicted tokens, we compute the

Original prompt: What is the capital of France?	
Character-Level Perturbations	
1. Insertion	What is the capital of rFrance?
2. Deletion	What is the cap _tal of France?
3. Replacement	What is the capital of rFrance?
4. Swapping	What is teh capital of France?
5. Repetition	Whatt is the capital of France?
6. Leetspeak	What is the c@pital of France?
7. Noise	What is the capital of Fra!nce?
8. Case Change	What is the capital oF France?
9. Emoji	What is the capital of France? 😊
Word-Level Perturbations	
10. Insertion	What is the capital city of France?
11. Deletion	What _ the capital of France?
12. Swapping	is What the capital of France?
13. Repetition	What What is the capital of France?
14. Slang	What is the capital of France rofl?
15. Translation	What is the capital of 法国?

Figure 2: Overview of our character-level and word-level input perturbations. Illustrated is an example where perturbations with intensity level 1 are applied to a standard question prompt.

216 *token-level entropy*, which corresponds to the Shannon entropy of the token distribution (Fomicheva
217 et al., 2020; Malinin & Gales, 2020):

$$218 H_t = - \sum_{k=1}^{|\mathcal{V}|} P_\theta(\mathbf{y}_k | \mathbf{y}_{1:t-1}, \mathbf{x}) \log P_\theta(\mathbf{y}_k | \mathbf{y}_{1:t-1}, \mathbf{x}), \quad (3)$$

219 measured across the entire vocabulary \mathcal{V} . Higher entropy corresponds to increased uncertainty in
220 the predicted next-token distribution, while lower entropy corresponds to increased confidence. To
221 quantify the model’s uncertainty in the correct next-token, we compute the *token-level log-likelihood*
222 of the ground-truth token \mathbf{y}_t^* as follows:

$$223 C_t^* = \log P_\theta(\mathbf{y}_t^* | \mathbf{y}_{1:t-1}^*, \mathbf{x}). \quad (4)$$

224 To assess how well-calibrated the model’s predicted token distributions are, we adopt the *Brier Score*
225 (Brier, 1950), and define the token-level calibration as:

$$226 \text{Brier}_t = \sum_{k=1}^{|\mathcal{V}|} (P_\theta(\mathbf{y}_k | \mathbf{y}_{1:t-1}, \mathbf{x}) - \mathbf{y}_k^*)^2, \quad (5)$$

227 which corresponds to the squared Euclidean distance between the predicted token distribution
228 $P_\theta(\mathbf{y} | \mathbf{y}_{1:t-1}, \mathbf{x})$ and the one-hot encoded reference token.

229 3.2 ROBUSTNESS TO INPUT PERTURBATIONS

230 In this work, we focus on natural, semantically-preserving perturbations commonly encountered in
231 typed digital communication, such as messaging or chat-based applications. We introduce character-
232 level and word-level perturbations to the input prompt \mathbf{x} . We provide an overview of all input
233 perturbations in Fig. 2. We design natural perturbations that are increasingly present in online
234 communication (Suhardianto et al., 2019; Moradi & Samwald, 2021; Hand et al., 2022; Ackerman
235 et al., 2024), but remain underexplored in the robustness evaluation of base and quantized LLMs. We
236 implement the following perturbations:

- 237 • *Emoji*: Emojis are increasingly integrated into the written language in interpersonal commu-
238 nication. Current digital communication is more likely to include emojis alongside text rather
239 than traditional emoticons (Hand et al., 2022). To evaluate the model’s robustness to emojis, we
240 perturb the input prompt by randomly inserting emoji characters.
- 241 • *Replacement*: We substitute characters with adjacent keyboard alternatives to simulate realistic
242 typos, using a keyboard layout mapping that maintains case sensitivity (Ackerman et al., 2024).
- 243 • *Slang*: Slang expressions are commonly used to communicate informally in online dialogues
244 (Suhardianto et al., 2019). To test the model’s sensitivity to informal internet language, we
245 introduce perturbations by randomly inserting slang expressions such as "lol", "rofl", and "IMO".
- 246 • *Insertion*: At the word level, we add contextually relevant words using a language model (Liu
247 et al., 2019) to predict insertions while preserving text coherence. At the character level, we
248 randomly insert characters.
- 249 • *Leetspeak*: We substitute characters with visually similar numerals or symbols (for example, we
250 replace 'b' with '6'). We provide additional examples in Table 3.
- 251 • *Translation*: To simulate the linguistic behavior of individuals with different languages, we
252 randomly translate words to six common languages. Contrary to the semantic-level translation
253 perturbation introduced in Zhu et al. (2024), we do not translate phrases back to English.
- 254 • *Deletion*: In the process of deletion, we only remove filler words (e.g., "and", "to", or "actually")
255 that are not crucial for preserving the semantics. For character deletion, we randomly delete
256 characters from the sequence. This perturbation simulates typos that are commonly observed in
257 informal or fast-paced writing (Flor et al., 2015).

258 We further design standard character-level and word-level perturbations such as swapping, repetition,
259 and case change (Moradi & Samwald, 2021; Ackerman et al., 2024). We note that Ackerman
260 et al. (2024) test many of the character-level perturbations in adversarial attack scenarios. However,
261 in our work, we focus on a set of non-adversarial perturbations that can be used to assess the

robustness of LLMs. Additional details on all perturbations are provided in Section B. We provide radar plots of the accuracy and AUCROC (Entropy) on the unperturbed and perturbed TriviaQA dataset across all 15 perturbations in Fig. 3. We use the full precision LLaMA-3-8B model and five corresponding quantized models. We show that 4-bit quantization does not degrade the performance under perturbations. For the reliability evaluation, we report the AUCROC (Entropy) scores, and show that quantization methods, including GPTQ (Frantar et al., 2022), AWQ (Lin et al., 2024a), and HQQ (Badri & Shaji, 2023), improve the reliability of the base model under natural perturbations.

3.3 SCALING TRENDS

Consider two models: (i) a model with K_1 parameters in P_1 -bit precision, and (ii) a model with K_2 parameters in P_2 -bit precision, such that $K_1P_1 = K_2P_2$. Although both models have equal total bit budgets, their reliability characteristics can differ significantly. In this paper, our goal is to characterize how reliability scales with the total number of bits. Using total model bits as a unit for comparison enables a fair model comparison across different parameter counts and bitwidths. We note that we do not propose a formal predictive law in the classical sense; i.e., a closed-form equation that predicts outcomes a priori before evaluation. In prior works (Dettmers & Zettlemoyer, 2023; Frantar et al., 2025), scaling laws often refer to empirical regularities observed in model behavior, as a function of model size, compute, or dataset size. These laws are typically fit to the observed data and used to characterize trends. We adopt the same empirical methodology: we empirically characterize consistent trends in reliability behavior as the total number of bits B scales, defined as the product of the number of model parameters and the weight precision (in bits). Consider a performance metric \mathcal{L} modeled using a *log quadratic scaling law* as follows:

$$\mathcal{L}(B) = a(\log(B))^2 + b\log(B) + c, \quad (6)$$

where $a, b, c \in \mathbb{R}$ are fitted coefficients. This formulation captures nonlinear trends in model performance as the model capacity increases, and generally provides a good fit, as shown in Section 4.

Why is total model bits a reasonable axis of comparison? Total model bits provide a unified basis for systematically studying trade-offs between model scale and quantization bitwidth. It is both convenient and easy to measure, while also correlating well with several practical efficiency metrics. In particular, total model bits directly reflect the storage memory and scale linearly with the inference memory. We further discuss in Section C how it relates to inference latency and throughput. Table 4 provides a quantitative comparison of multiple efficiency metrics for models from the Qwen (Yang et al., 2025) family with comparable total bit budgets.

4 RELIABILITY ASSESSMENT OF QUANTIZED LLMs

We conduct a comprehensive evaluation of the reliability of quantized LLMs both on unperturbed and perturbed input prompts, across different model scales, families, and precisions. We address the following questions: How does the downstream task performance scale as a function of total model bits? Do the reliability scalings exhibit different trends? What is the optimal precision for trading off reliability and efficiency? Additionally, we conduct ablation studies to investigate whether these scaling behaviors persist across model families and benchmarks.

4.1 EXPERIMENTAL SETTING

Datasets: We consider commonly used benchmarks for evaluating the uncertainty quantification in LLMs across NLG tasks (Lin et al., 2023; Kuhn et al., 2023): **TriviaQA** (Joshi et al., 2017) and **CoQA** (Reddy et al., 2019). TriviaQA (Joshi et al., 2017) evaluates factual knowledge retrieval with question-answer pairs sourced from trivia competitions. It spans diverse knowledge domains, including history, literature, science, geography, and popular culture. CoQA (Reddy et al., 2019) (Conversational Question Answering) evaluates contextual understanding through multi-turn conversational exchanges. The dataset consists of conversations from seven diverse domains, including literature, news, and science. Additionally, we evaluate on **CommonsenseQA** (Talmor et al., 2018), a multiple-choice question-answering dataset designed to assess commonsense knowledge and reasoning capabilities, where the goal is to provide a single answer from five possible answer choices. To assess the language modeling capabilities, we evaluate on **WikiText-2** (Merity et al., 2016), **PTB** (Marcus et al., 1993),

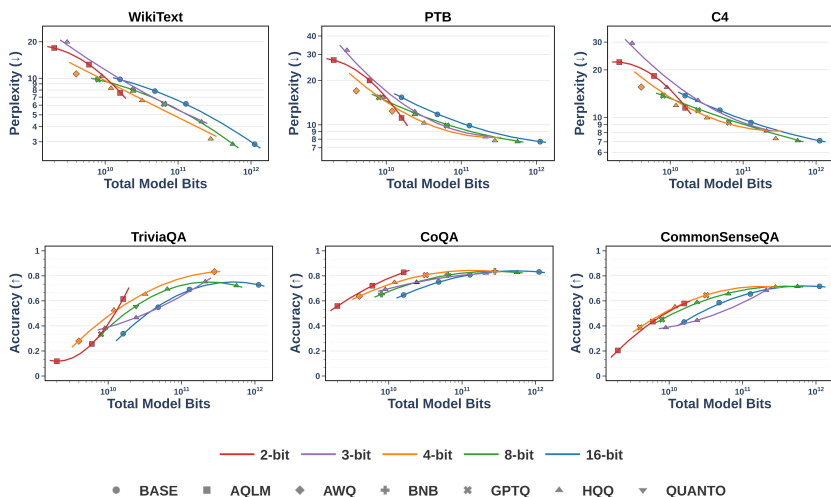


Figure 4: Scalings of the perplexity (**top**) and accuracy (**bottom**). The performance steadily improves with the total number of model bits. 4-bit models offer the best perplexity-efficiency and accuracy-efficiency trade-off given a fixed number of total model bits.

and **C4** (Raffel et al., 2020). Additional details on the datasets are presented in Section A.2. We extend the evaluation to additional benchmarks to assess the emergent abilities of base and quantized models on in-context learning and instruction-following tasks, as well as other NLP tasks such as reasoning and comprehension in Section D. A summary of all evaluated benchmarks is provided in Table 2.

Base and quantized LLMs: We consider four base pre-trained models (Grattafiori et al., 2024), including two models from the LLaMA-3.2 family: LLaMA-3.2-1B and LLaMA-3.2-3B, and two models from the LLaMA-3 family: LLaMA-3-8B and LLaMA-3-70B. For the quantization, we consider six state-of-the-art quantization methods across various bit precision levels, ranging from 2 bits to 8 bits. These approaches include BitsandBytes (Dettmers et al., 2022), AWQ (Lin et al., 2024a), GPTQ (Frantar et al., 2022), HQQ (Badri & Shaji, 2023; 2024), Quanto (Team, 2023), and AQLM (Egiazarian et al., 2024; Malinovskii et al., 2024). For the 2-bit quantization using AQLM, we adopt the AQLM-PV variant, corresponding to the quantized model with additional fine-tuning for improved performance. We adopt the bitwidths supported by the respective reference implementations of each quantization method. A complete list of all base models, quantized models, and corresponding precision levels is presented in Section A.1. To better capture performance trends, we fit log-quadratic functions as outlined in Section 3.3.

4.2 BIT-LEVEL SCALING TRENDS

Downstream task performance scalings. We evaluate the downstream performance of base and quantized LLMs on *unperturbed* (i.e., original) datasets. In Fig. 4, we present the scaling behavior of the perplexity and the accuracy across different quantization levels and model sizes. First, we observe that the downstream task performance improves with increased total model bits. Second, we find that reducing the precision from 16 to 4 bits, for a given total bit budget, consistently improves both the perplexity and the accuracy across all evaluated datasets. However, this trend is reversed if we further decrease the precision to 3 bits and 2 bits, aligning with previous observations in Hong et al. (2024); Dettmers & Zettlemoyer (2023). We note that the 2-bit quantization using AQLM (Egiazarian et al., 2024; Malinovskii et al., 2024) achieves a relatively good performance in the low-bit regime on CoQA and CommonsenseQA. For the 3-bit quantization, HQQ (Badri & Shaji, 2023) achieves the best performance. For the 4-bit setting, both HQQ (Badri & Shaji, 2023) and AWQ (Lin et al., 2024a) offer the best performance-efficiency trade-off.

378
379
380
381
382
383
384
385
386
387
388
389
390
391
392
393
394
395
396
397
398
399
400
401
402
403
404
405
406
407
408
409
410
411
412
413
414
415
416
417
418
419
420
421
422
423
424
425
426
427
428
429
430
431

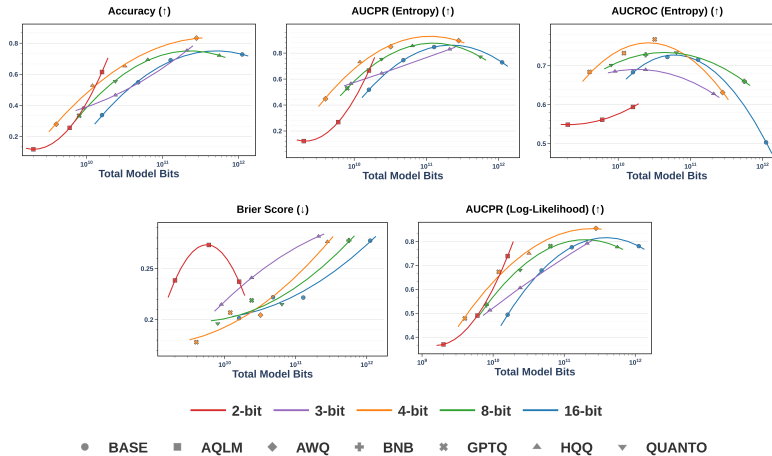


Figure 5: Zero-shot performance and reliability scaling trends on the TriviaQA dataset. We use four base models from the LLaMA family and six state-of-the-art quantization techniques.

Takeaways:

- Performance scaling trends are monotonic in the total number of model bits.
- For a fixed total bit budget, the performance improves as the precision decreases from 16 to 4 bits; this trend reverses below 4 bits. Therefore, 4-bit is the optimal precision to achieve the best zero-shot performance.

Reliability scaling trends. To characterize the reliability of base and quantized models, we present the scaling behavior of the accuracy and the reliability metrics on TriviaQA (Joshi et al., 2017) in Fig. 5. We further provide the scalings on the *perturbed* TriviaQA dataset in Fig. 6. We average the metrics across all 15 perturbations and provide a qualitative comparison for two different perturbation intensities. On the one hand, accuracy increases under both unperturbed and perturbed prompts with the total number of model bits. Additionally, 4-bit models offer the strongest robust accuracy for a fixed bit budget. We note that the 3-bit HQQ quantization of the LLaMA-3-70B model achieves an accuracy comparable to its 4-bit counterpart. On the other hand, bit-level reliability scalings are not linear. More specifically, larger models exhibit lower AUCROC (Entropy), indicating reduced reliability under perturbations. Extreme 2-bit quantization methods exhibit different scaling trends than moderate precisions. While 4-bit, 8-bit, and 16-bit models have worse uncertainty estimates and calibration in the large-bit regime, the reliability of 2-bit models improves with model scale. Additional results on the perturbed benchmarks are provided in Section E.

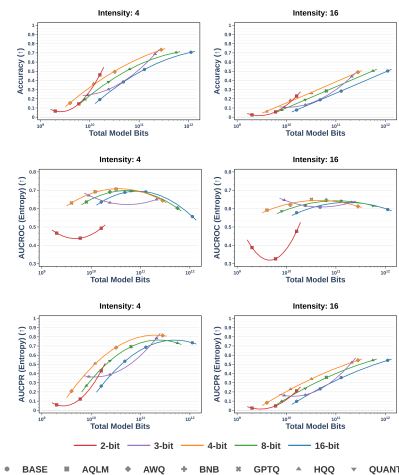
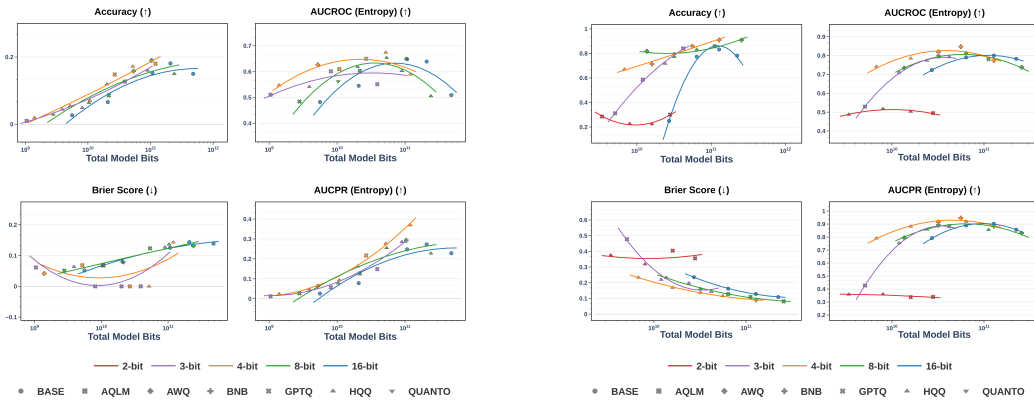


Figure 6: Bit-level scalings on the **perturbed** TriviaQA dataset, averaged over all 15 perturbations.

Takeaways:

- For a fixed total bit budget, 4-bit models achieve the highest *robust accuracy* under both character-level and word-level perturbations.
- For a fixed bitwidth, *robust accuracy* increases with model scale.
- *Reliability* generally improves as the bitwidth is reduced from 16 to 4 bits.
- Across different model scales and bitwidth, 4-bit precision consistently maximizes the reliability under natural perturbations.

432
433
434
435
436
437
438
439
440
441
442
443
444
445
446
447
448
449
450
451
452
453
454
455
456
457
458
459
460
461
462
463
464
465
466
467
468
469
470
471
472
473
474
475
476
477
478
479
480
481
482
483
484
485



(a) Scaling trends of OPT models on TriviaQA (Joshi et al., 2017).

(b) Scaling trends of Qwen3 models on CEval (Huang et al., 2023).

Figure 7: Bit-level inference scaling trends of full-precision and quantized models on OPT and Qwen models.

We explain the peak occurring at 4-bit for the reliability scalings with 2 regimes: **Below 4-bit precision**, 2-bit and 3-bit quantized models lose the predictive performance for a low total bit budget across various datasets (see Fig. 6), which can directly contribute to diminished reliability. **Above 4-bit precision**, 8-bit and 16-bit models tend to be overconfident in their predictions, which leads to an increase in the calibration error, as shown through the Brier Score scalings. Both larger 8-bit and 16-bit models have worse AUCPR(Entropy) scores and lower likelihood in the ground-truth answers compared to the 4-bit quantized models. Prior works (Yang et al., 2024; Sun et al., 2025) show that larger LLMs tend to be overconfident and less reliable, which we hypothesize contributes to the non-linear trend observed as bitwidth increases. **The peak at 4-bit precision** offers a sweet spot where the model retains sufficient representational capacity while benefiting from quantization-induced regularization, striking a balance between quality degradation and overconfidence; an effect that is consistently observed across architectures, datasets, and setups (see Section D and Section E).

Are the scaling trends consistent across diverse model architectures? We extend our analysis beyond the LLaMA-3 family to include models from OPT (Zhang et al., 2022) and Qwen3 (Yang et al., 2025) series. For OPT, we evaluate six base models with parameter counts of 350M, 1.3B, 2.7B, 13B, and 30B, and present qualitative results in Fig. 7a. For Qwen3, we consider models of sizes 4B, 8B, 14B, and 32B, and present results in Fig. 7b. Across different architectures, we observe a consistent 4-bit sweet spot: 4-bit quantization generally achieves the best trade-off between accuracy, reliability, and efficiency. Moreover, the scaling behavior aligns with our earlier findings. Interestingly, for Qwen models, we find that the extreme 3-bit quantization of moderate-to-large models yields favorable performance. For OPT models, HQQ and GPTQ exhibit the best performance among 4-bit quantization methods, with GPTQ achieving the best results among 3-bit quantizations. For Qwen models, HQQ and BitsandBytes outperform other PTQ approaches in the 4-bit setting, whereas GPTQ and HQQ provide the best performance under 3-bit compression. Additional evaluations on widely used benchmarks for Qwen models are presented in Section D.

How do pruning strategies affect the reliability scaling trends of LLMs? While our primary focus is to characterize the scaling behavior of PTQ techniques across various model sizes and bitwidths, motivated by their methodological diversity and growing adoption, we also examine pruning, another widely used post-training compression strategy. In particular, we evaluate two state-of-the-art pruning techniques for LLMs: Wanda (Sun et al., 2023) and SparseGPT (Frantar & Alistarh, 2023). We prune four base LLaMA models at sparsity levels of 0.1, 0.3, 0.5, and additionally apply semi-structured 2:4 pruning. The N:M sparsity pattern enforces that only N weights remain non-zero within each block of M consecutive weights. Unlike unstructured pruning, N:M pruning can provide actual hardware acceleration. The corresponding scaling trends are presented in Fig. 8, where base models have zero sparsity. We find that as the sparsity increases, both performance and reliability degrade. While unstructured pruning at low sparsity levels can preserve a performance close to that of their base counterparts, it does not yield substantial gains as observed with 4-bit quantization. This is consistent with prior findings (Harma et al., 2024), which suggest that quantization-induced error

486
487
488
489
490
491
492
493
494
495
496
497
498
499
500
501
502
503
504
505
506
507
508
509
510
511
512
513
514
515
516
517
518
519
520
521
522
523
524
525
526
527
528
529
530
531
532
533
534
535
536
537
538
539

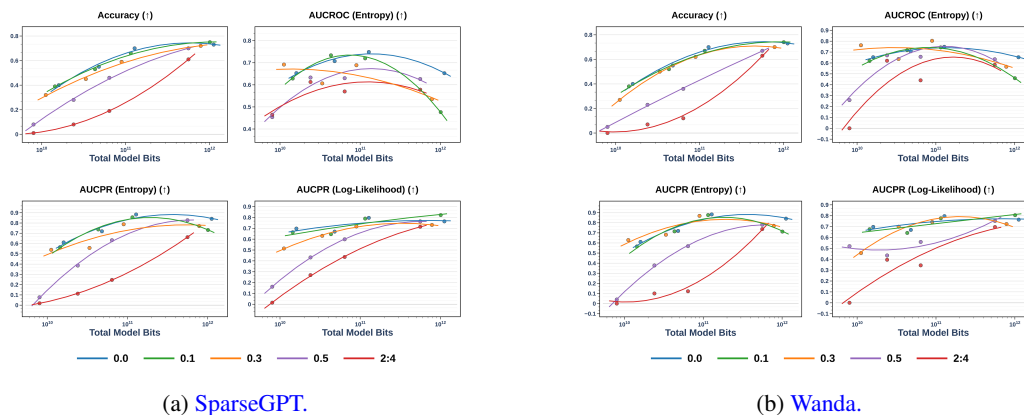


Figure 8: Reliability scaling trends of models pruned using SparseGPT and Wanda to different sparsity patterns.

is lower than that introduced by sparsification; and therefore, quantized LLMs generally outperform pruned LLMs. While both 50% sparse and semi-structured models exhibit noticeable degradation in reliability, we find that their performance improves significantly as model scale increases. A similar trend is observed for 3-bit quantized models, as shown in Fig. 6.

4.3 DISCUSSION AND LIMITATIONS

In this paper, we provide the first comprehensive reliability evaluation of base and quantized models by studying the underlying bit-level scaling trends across different model scales and bitwidths. While prior work Jaiswal et al. (2023); Dutta et al. (2024); Dettmers & Zettlemoyer (2023) focus exclusively on zero-shot performance of quantized models, we argue that the downstream task performance is insufficient. Notably, although the performance scales linearly with the total number of bits, with 4-bit quantization generally yielding the highest accuracy, the reliability trends are not linear: A peak occurs for 4-bit models, suggesting that a favorable reliability-efficiency trade-off can be achieved without resorting to the largest model or the highest precision. We further examine the robustness of base and quantized models under natural input perturbations and reveal that 4-bit quantization can enhance the robustness to semantically preserving perturbations that occur in typed digital communication. Our findings are consistent across diverse model architectures and datasets. We further examine the scalings of two pruning methods (Sun et al., 2023; Frantar & Alistarh, 2023), and find that sparsification does not offer significant reliability gains as observed with quantization, aligning with recent findings (Harma et al., 2024).

For future work, exploring how model calibration, multi-shot prompting, and model fine-tuning can affect the reliability scalings of quantized LLMs is crucial. Additionally, an interesting direction is studying which hyperparameters improve the reliability scalings for a specific number of model parameters and bit precision. We focus on post-training quantization approaches as they are widely adopted. Future work can extend this study to other compression approaches, such as Quantization-Aware Training (QAT) techniques, which may reveal different trends. This is particularly interesting given the potential of QAT to improve the performance of extreme quantization (Ma et al., 2024).

5 CONCLUSION

We present a comprehensive evaluation of quantized LLMs across key reliability dimensions, focusing specifically on uncertainty and robustness to semantically-preserving input perturbations. While prior studies have primarily emphasized evaluating the accuracy of quantized models on standard benchmarks, our findings reveal that this narrow focus overlooks critical safety considerations. By studying reliability scaling trends, we show that reliability does not necessarily scale monotonically with the total number of model bits. An optimal reliability-efficiency trade-off can be achieved without resorting to the highest precision or quantizing the largest base model. We emphasize the potential of quantization to enhance the reliability of models, making it a promising direction for deploying trustworthy LLMs in practical settings.

Reproducibility Statement For reproducibility, we list all the base models used in our evaluation, as well as the corresponding quantization methods and their bitwidths in Section A.1. We further provide details on the evaluation datasets and experimental setup in Section A.2. We provide a detailed description for the implementation of the character-level and word-level input perturbations in Section B. We specify how we construct the scaling laws in Section 3.3. In addition, we make the code available as part of the supplementary material with the submission.

REFERENCES

- Samuel Ackerman, Ella Rabinovich, Eitan Farchi, and Ateret Anaby Tavor. A novel metric for measuring the robustness of large language models in non-adversarial scenarios. In Yaser Al-Onaizan, Mohit Bansal, and Yun-Nung Chen (eds.), *Findings of the Association for Computational Linguistics: EMNLP 2024*, pp. 2794–2802, Miami, Florida, USA, November 2024. Association for Computational Linguistics. doi: 10.18653/v1/2024.findings-emnlp.158. URL <https://aclanthology.org/2024.findings-emnlp.158/>.
- Saleh Ashkboos, Amirkeivan Mohtashami, Maximilian L. Croci, Bo Li, Pashmina Cameron, Martin Jaggi, Dan Alistarh, Torsten Hoefler, and James Hensman. Quarot: Outlier-free 4-bit inference in rotated LLMs. In *The Thirty-eighth Annual Conference on Neural Information Processing Systems*, 2024. URL <https://openreview.net/forum?id=dfqsW38v1X>.
- Hicham Badri and Appu Shaji. Half-Quadratic Quantization of Large Machine Learning Models, November 2023. URL https://mobiusml.github.io/hqq_blog/.
- Hicham Badri and Appu Shaji. Towards 1-bit Machine Learning Models, March 2024. URL https://mobiusml.github.io/1bit_blog/.
- Yonatan Bisk, Rowan Zellers, Jianfeng Gao, Yejin Choi, et al. Piqa: Reasoning about physical commonsense in natural language. In *Proceedings of the AAAI conference on artificial intelligence*, pp. 7432–7439, 2020.
- Glenn W Brier. Verification of forecasts expressed in terms of probability. *Monthly weather review*, 78(1):1–3, 1950.
- Kejia Chen, Jiawen Zhang, Jiacong Hu, Yu Wang, Jian Lou, Zunlei Feng, and Mingli Song. Q-resafe: Assessing safety risks and quantization-aware safety patching for quantized large language models. *arXiv preprint arXiv:2506.20251*, 2025a.
- Mengzhao Chen, Wenqi Shao, Peng Xu, Jiahao Wang, Peng Gao, Kaipeng Zhang, and Ping Luo. Efficientqat: Efficient quantization-aware training for large language models. In *Proceedings of the 63rd Annual Meeting of the Association for Computational Linguistics (Volume 1: Long Papers)*, pp. 10081–10100, 2025b.
- Peter Clark, Isaac Cowhey, Oren Etzioni, Tushar Khot, Ashish Sabharwal, Carissa Schoenick, and Oyvind Tafjord. Think you have solved question answering? try arc, the ai2 reasoning challenge. *arXiv preprint arXiv:1803.05457*, 2018.
- Tim Dettmers and Luke Zettlemoyer. The case for 4-bit precision: k-bit inference scaling laws. In *International Conference on Machine Learning*, pp. 7750–7774. PMLR, 2023.
- Tim Dettmers, Artidoro Pagnoni, Alexander Borzunov, and Mike Lewis. bitsandbytes: Efficient CUDA Primitives for 8-bit and 4-bit Neural Network Quantization. <https://github.com/bitsandbytes-foundation/bitsandbytes>, 2022. Accessed: March 2025.
- Peiran Dong, Haowei Li, and Song Guo. Durable quantization conditioned misalignment attack on large language models. In *The Thirteenth International Conference on Learning Representations*, 2025.
- Abhinav Dutta, Sanjeev Krishnan, Nipun Kwatra, and Ramachandran Ramjee. Accuracy is not all you need. *arXiv preprint arXiv:2407.09141*, 2024.

- 594 Vage Egiazarian, Andrei Panferov, Denis Kuznedelev, Elias Frantar, Artem Babenko, and Dan
595 Alistarh. Extreme compression of large language models via additive quantization. *arXiv preprint*
596 *arXiv:2401.06118*, 2024.
- 597 M Flor, Y Futagi, M Lopez, and M Mulholland. Patterns of misspellings in l2 and l1 english: A view
598 from the ets spelling corpus. *bergen language and linguistics studies*, 6, 107–132, 2015.
- 600 Marina Fomicheva, Shuo Sun, Lisa Yankovskaya, Frédéric Blain, Francisco Guzmán, Mark Fishel,
601 Nikolaos Aletras, Vishrav Chaudhary, and Lucia Specia. Unsupervised quality estimation for
602 neural machine translation. *Transactions of the Association for Computational Linguistics*, 8:
603 539–555, 2020.
- 604 Elias Frantar and Dan Alistarh. Sparsegpt: Massive language models can be accurately pruned in
605 one-shot. In *International Conference on Machine Learning*, pp. 10323–10337. PMLR, 2023.
- 606 Elias Frantar, Saleh Ashkboos, Torsten Hoefler, and Dan Alistarh. Gptq: Accurate post-training
607 quantization for generative pre-trained transformers. *arXiv preprint arXiv:2210.17323*, 2022.
- 608 Elias Frantar, Utku Evci, Wonpyo Park, Neil Houlsby, and Dan Alistarh. Compression scaling laws:
609 Unifying sparsity and quantization. *arXiv preprint arXiv:2502.16440*, 2025.
- 610 Aaron Grattafiori, Abhimanyu Dubey, Abhinav Jauhri, Abhinav Pandey, Abhishek Kadian, Ahmad
611 Al-Dahle, Aiesha Letman, Akhil Mathur, Alan Schelten, Alex Vaughan, et al. The llama 3 herd of
612 models. *arXiv preprint arXiv:2407.21783*, 2024.
- 613 Yuxian Gu, Li Dong, Furu Wei, and Minlie Huang. Minillm: Knowledge distillation of large language
614 models. *arXiv preprint arXiv:2306.08543*, 2023.
- 615 Christopher J Hand, Cassandra Burd, Alex Oliver, and Christopher M Robus. Interactions between
616 text content and emoji types determine perceptions of both messages and senders. *Computers in*
617 *human behavior reports*, 8:100242, 2022.
- 618 Simla Burcu Harma, Ayan Chakraborty, Elizaveta Kostenok, Danila Mishin, Dongho Ha, Babak
619 Falsafi, Martin Jaggi, Ming Liu, Yunho Oh, Suvinay Subramanian, et al. Effective interplay
620 between sparsity and quantization: From theory to practice. *arXiv preprint arXiv:2405.20935*,
621 2024.
- 622 Dan Hendrycks, Collin Burns, Steven Basart, Andy Zou, Mantas Mazeika, Dawn Song, and
623 Jacob Steinhardt. Measuring massive multitask language understanding. *arXiv preprint*
624 *arXiv:2009.03300*, 2020.
- 625 Danny Hernandez, Jared Kaplan, Tom Henighan, and Sam McCandlish. Scaling laws for transfer.
626 *arXiv preprint arXiv:2102.01293*, 2021.
- 627 Jordan Hoffmann, Sebastian Borgeaud, Arthur Mensch, Elena Buchatskaya, Trevor Cai, Eliza
628 Rutherford, Diego de Las Casas, Lisa Anne Hendricks, Johannes Welbl, Aidan Clark, et al.
629 Training compute-optimal large language models. *arXiv preprint arXiv:2203.15556*, 2022.
- 630 Junyuan Hong, Jinhao Duan, Chenhui Zhang, Zhangheng Li, Chulin Xie, Kelsey Lieberman, James
631 Diffenderfer, Brian Bartoldson, Ajay Jaiswal, Kaidi Xu, et al. Decoding compressed trust: Scruti-
632 nizing the trustworthiness of efficient llms under compression. *arXiv preprint arXiv:2403.15447*,
633 2024.
- 634 Yuzhen Huang, Yuzhuo Bai, Zhihao Zhu, Junlei Zhang, Jinghan Zhang, Tangjun Su, Junteng Liu,
635 Chuancheng Lv, Yikai Zhang, Yao Fu, et al. C-eval: A multi-level multi-discipline chinese
636 evaluation suite for foundation models. *Advances in Neural Information Processing Systems*, 36:
637 62991–63010, 2023.
- 638 Ajay Jaiswal, Zhe Gan, Xianzhi Du, Bowen Zhang, Zhangyang Wang, and Yinfei Yang. Compressing
639 llms: The truth is rarely pure and never simple. *arXiv preprint arXiv:2310.01382*, 2023.
- 640 Zhengbao Jiang, Jun Araki, Haibo Ding, and Graham Neubig. How can we know when language
641 models know? on the calibration of language models for question answering. *Transactions of the*
642 *Association for Computational Linguistics*, 9:962–977, 2021.

- 648 Mandar Joshi, Eunsol Choi, Daniel S Weld, and Luke Zettlemoyer. Triviaqa: A large scale distantly
649 supervised challenge dataset for reading comprehension. *arXiv preprint arXiv:1705.03551*, 2017.
650
- 651 Saurav Kadavath, Tom Conerly, Amanda Askell, Tom Henighan, Dawn Drain, Ethan Perez, Nicholas
652 Schiefer, Zac Hatfield-Dodds, Nova DasSarma, Eli Tran-Johnson, et al. Language models (mostly)
653 know what they know. *arXiv preprint arXiv:2207.05221*, 2022.
654
- 655 Jared Kaplan, Sam McCandlish, Tom Henighan, Tom B Brown, Benjamin Chess, Rewon Child, Scott
656 Gray, Alec Radford, Jeffrey Wu, and Dario Amodei. Scaling laws for neural language models.
657 *arXiv preprint arXiv:2001.08361*, 2020.
- 658 Sanyam Kapoor, Nate Gruver, Manley Roberts, Arka Pal, Samuel Dooley, Micah Goldblum, and
659 Andrew Wilson. Calibration-tuning: Teaching large language models to know what they don't
660 know. In *Proceedings of the 1st Workshop on Uncertainty-Aware NLP (UncertainNLP 2024)*, pp.
661 1–14, 2024.
662
- 663 Ranganath Krishnan, Piyush Khanna, and Omesh Tickoo. Enhancing trust in large language models
664 with uncertainty-aware fine-tuning. *arXiv preprint arXiv:2412.02904*, 2024.
665
- 666 Lorenz Kuhn, Yarin Gal, and Sebastian Farquhar. Semantic uncertainty: Linguistic invariances for
667 uncertainty estimation in natural language generation. *arXiv preprint arXiv:2302.09664*, 2023.
668
- 669 Tanishq Kumar, Zachary Ankner, Benjamin F Spector, Blake Bordelon, Niklas Muennighoff, Man-
670 sheej Paul, Cengiz Pehlevan, Christopher Ré, and Aditi Raghunathan. Scaling laws for precision.
671 *arXiv preprint arXiv:2411.04330*, 2024.
672
- 673 Guokun Lai, Qizhe Xie, Hanxiao Liu, Yiming Yang, and Eduard Hovy. Race: Large-scale reading
674 comprehension dataset from examinations. *arXiv preprint arXiv:1704.04683*, 2017.
675
- 676 Shiyao Li, Xuefei Ning, Luning Wang, Tengxuan Liu, Xiangsheng Shi, Shengen Yan, Guohao Dai,
677 Huazhong Yang, and Yu Wang. Evaluating quantized large language models. *arXiv preprint*
678 *arXiv:2402.18158*, 2024.
679
- 680 Chen Liang, Simiao Zuo, Qingru Zhang, Pengcheng He, Weizhu Chen, and Tuo Zhao. Less is more:
681 Task-aware layer-wise distillation for language model compression. In *International Conference*
682 *on Machine Learning*, pp. 20852–20867. PMLR, 2023.
683
- 684 Chin-Yew Lin and Franz Josef Och. Automatic evaluation of machine translation quality using
685 longest common subsequence and skip-bigram statistics. In *Proceedings of the 42nd annual*
686 *meeting of the association for computational linguistics (ACL-04)*, pp. 605–612, 2004.
687
- 688 Ji Lin, Jiaming Tang, Haotian Tang, Shang Yang, Wei-Ming Chen, Wei-Chen Wang, Guangxuan
689 Xiao, Xingyu Dang, Chuang Gan, and Song Han. Awq: Activation-aware weight quantization for
690 on-device llm compression and acceleration. *Proceedings of Machine Learning and Systems*, 6:
691 87–100, 2024a.
692
- 693 Yujun Lin, Haotian Tang, Shang Yang, Zhekai Zhang, Guangxuan Xiao, Chuang Gan, and Song Han.
694 QServe: W4A8KV4 Quantization and System Co-design for Efficient LLM Serving, May 2024b.
695 URL <http://arxiv.org/abs/2405.04532>. arXiv:2405.04532 [cs].
696
- 697 Zhen Lin, Shubhendu Trivedi, and Jimeng Sun. Generating with confidence: Uncertainty quantifica-
698 tion for black-box large language models. *arXiv preprint arXiv:2305.19187*, 2023.
699
- 700 Yinhan Liu, Myle Ott, Naman Goyal, Jingfei Du, Mandar Joshi, Danqi Chen, Omer Levy, Mike
701 Lewis, Luke Zettlemoyer, and Veselin Stoyanov. Roberta: A robustly optimized bert pretraining
approach. *arXiv preprint arXiv:1907.11692*, 2019.
- Zechun Liu, Barlas Oguz, Changsheng Zhao, Ernie Chang, Pierre Stock, Yashar Mehdad, Yangyang
Shi, Raghuraman Krishnamoorthi, and Vikas Chandra. Llm-qat: Data-free quantization aware
training for large language models. In *Findings of the Association for Computational Linguistics:*
ACL 2024, pp. 467–484, 2024.

- 702 Shuming Ma, Hongyu Wang, Lingxiao Ma, Lei Wang, Wenhui Wang, Shaohan Huang, Lifeng Dong,
703 Ruiping Wang, Jilong Xue, and Furu Wei. The era of 1-bit llms: All large language models are in
704 1.58 bits. *arXiv preprint arXiv:2402.17764*, 1(4), 2024.
- 705
706 Andrey Malinin and Mark Gales. Uncertainty estimation in autoregressive structured prediction.
707 *arXiv preprint arXiv:2002.07650*, 2020.
- 708 Vladimir Malinovskii, Denis Mazur, Ivan Ilin, Denis Kuznedelev, Konstantin Pavlovich Burlachenko,
709 Kai Yi, Dan Alistarh, and Peter Richtárik. PV-tuning: Beyond straight-through estimation for
710 extreme LLM compression. In *The Thirty-eighth Annual Conference on Neural Information*
711 *Processing Systems*, 2024. URL <https://openreview.net/forum?id=YvA8UF0I37>.
- 712
713 Mitch Marcus, Beatrice Santorini, and Mary Ann Marcinkiewicz. Building a large annotated corpus
714 of english: The penn treebank. *Computational linguistics*, 19(2):313–330, 1993.
- 715
716 Stephen Merity, Caiming Xiong, James Bradbury, and Richard Socher. Pointer sentinel mixture
717 models. *arXiv preprint arXiv:1609.07843*, 2016.
- 718
719 Milad Moradi and Matthias Samwald. Evaluating the robustness of neural language models to input
720 perturbations. *arXiv preprint arXiv:2108.12237*, 2021.
- 721
722 Colin Raffel, Noam Shazeer, Adam Roberts, Katherine Lee, Sharan Narang, Michael Matena, Yanqi
723 Zhou, Wei Li, and Peter J Liu. Exploring the limits of transfer learning with a unified text-to-text
724 transformer. *Journal of machine learning research*, 21(140):1–67, 2020.
- 725
726 Siva Reddy, Danqi Chen, and Christopher D Manning. Coqa: A conversational question answering
727 challenge. *Transactions of the Association for Computational Linguistics*, 7:249–266, 2019.
- 728
729 Ben Sorscher, Robert Geirhos, Shashank Shekhar, Surya Ganguli, and Ari Morcos. Beyond neural
730 scaling laws: beating power law scaling via data pruning. *Advances in Neural Information*
731 *Processing Systems*, 35:19523–19536, 2022.
- 732
733 Suhardianto Suhardianto et al. Colloquial, slang and transformational language: comparative study.
734 *Jurnal Basis*, 6(1):105–118, 2019.
- 735
736 Fengfei Sun, Ningke Li, Kailong Wang, and Lorenz Goette. Large language models are overconfident
737 and amplify human bias. *arXiv preprint arXiv:2505.02151*, 2025.
- 738
739 Mingjie Sun, Zhuang Liu, Anna Bair, and J Zico Kolter. A simple and effective pruning approach for
740 large language models. *arXiv preprint arXiv:2306.11695*, 2023.
- 741
742 Alon Talmor, Jonathan Herzig, Nicholas Lourie, and Jonathan Berant. Commonsenseqa: A question
743 answering challenge targeting commonsense knowledge. *arXiv preprint arXiv:1811.00937*, 2018.
- 744
745 Gemma Team, Thomas Mesnard, Cassidy Hardin, Robert Dadashi, Surya Bhupatiraju, Shreya Pathak,
746 Laurent Sifre, Morgane Rivière, Mihir Sanjay Kale, Juliette Love, et al. Gemma: Open models
747 based on gemini research and technology. *arXiv preprint arXiv:2403.08295*, 2024.
- 748
749 Hugging Face Team. Optimum quanto: A pytorch quantization backend for optimum. <https://huggingface.co/docs/optimum/quanto/index>, 2023. Accessed: March 2025.
- 750
751 Hugo Touvron, Louis Martin, Kevin Stone, Peter Albert, Amjad Almahairi, Yasmine Babaei, Nikolay
752 Bashlykov, Soumya Batra, Prajjwal Bhargava, Shruti Bhosale, et al. Llama 2: Open foundation
753 and fine-tuned chat models. *arXiv preprint arXiv:2307.09288*, 2023.
- 754
755 Haoyu Wang, Guozheng Ma, Cong Yu, Ning Gui, Linrui Zhang, Zhiqi Huang, Suwei Ma, Yongzhe
756 Chang, Sen Zhang, Li Shen, Xueqian Wang, Peilin Zhao, and Dacheng Tao. Are large language
757 models really robust to word-level perturbations? *Submitted to Transactions on Machine Learning*
758 *Research*, 2024. URL <https://openreview.net/forum?id=BMKJEGNMcz>. Rejected.
- 759
760 Jason Wei, Yi Tay, Rishi Bommasani, Colin Raffel, Barret Zoph, Sebastian Borgeaud, Dani Yogatama,
761 Maarten Bosma, Denny Zhou, Donald Metzler, et al. Emergent abilities of large language models.
762 *arXiv preprint arXiv:2206.07682*, 2022.

- 756 Thomas Wolf, Lysandre Debut, Victor Sanh, Julien Chaumond, Clement Delangue, Anthony Moi,
757 Pierric Cistac, Tim Rault, Rémi Louf, Morgan Funtowicz, et al. Huggingface’s transformers:
758 State-of-the-art natural language processing. *arXiv preprint arXiv:1910.03771*, 2019.
759
- 760 Yuzhuang Xu, Xu Han, Zonghan Yang, Shuo Wang, Qingfu Zhu, Zhiyuan Liu, Weidong Liu, and
761 Wanxiang Che. Onebit: Towards extremely low-bit large language models. *Advances in Neural
762 Information Processing Systems*, 37:66357–66382, 2024a.
- 763 Zhichao Xu, Ashim Gupta, Tao Li, Oliver Bentham, and Vivek Srikumar. Beyond perplexity:
764 Multi-dimensional safety evaluation of llm compression. *arXiv preprint arXiv:2407.04965*, 2024b.
765
- 766 An Yang, Anfeng Li, Baosong Yang, Beichen Zhang, Binyuan Hui, Bo Zheng, Bowen Yu, Chang
767 Gao, Chengen Huang, Chenxu Lv, et al. Qwen3 technical report. *arXiv preprint arXiv:2505.09388*,
768 2025.
- 769 Haoyan Yang, Yixuan Wang, Xingyin Xu, Hanyuan Zhang, and Yirong Bian. Can we trust llms?
770 mitigate overconfidence bias in llms through knowledge transfer. *arXiv preprint arXiv:2405.16856*,
771 2024.
- 772 Fanghua Ye, Mingming Yang, Jianhui Pang, Longyue Wang, Derek Wong, Emine Yilmaz, Shuming
773 Shi, and Zhaopeng Tu. Benchmarking llms via uncertainty quantification. *Advances in Neural
774 Information Processing Systems*, 37:15356–15385, 2024.
775
- 776 Rowan Zellers, Ari Holtzman, Yonatan Bisk, Ali Farhadi, and Yejin Choi. Hellaswag: Can a machine
777 really finish your sentence? *arXiv preprint arXiv:1905.07830*, 2019.
- 778 Susan Zhang, Stephen Roller, Naman Goyal, Mikel Artetxe, Moya Chen, Shuohui Chen, Christopher
779 Dewan, Mona Diab, Xian Li, Xi Victoria Lin, et al. Opt: Open pre-trained transformer language
780 models. *arXiv preprint arXiv:2205.01068*, 2022.
781
- 782 Kaijie Zhu, Jindong Wang, Jiaheng Zhou, Zichen Wang, Hao Chen, Yidong Wang, Linyi Yang,
783 Wei Ye, Yue Zhang, Neil Gong, and Xing Xie. Promptrobust: Towards evaluating the robustness
784 of large language models on adversarial prompts. In *Proceedings of the 1st ACM Workshop
785 on Large AI Systems and Models with Privacy and Safety Analysis*, LAMPS ’24, pp. 57–68,
786 New York, NY, USA, 2024. Association for Computing Machinery. ISBN 9798400712098. doi:
787 10.1145/3689217.3690621. URL <https://doi.org/10.1145/3689217.3690621>.
788
789
790
791
792
793
794
795
796
797
798
799
800
801
802
803
804
805
806
807
808
809

A ADDITIONAL DETAILS ON THE EXPERIMENTAL SETTING

A.1 QUANTIZATION METHODS

We present the complete list of base models and quantized models used in our evaluations in Table 1. We consider different quantization methods, including BNB (Dettmers et al., 2022), AWQ (Lin et al., 2024a), GPTQ (Frantar et al., 2022), HQQ (Badri & Shaji, 2023; 2024), Quanto (Team, 2023), AQLM (Egiazarian et al., 2024; Malinovskii et al., 2024), QuaRot (Ashkboos et al., 2024), and QoQ (Lin et al., 2024b), applied across 4 LLaMA models from the LLaMA-3 family. Not all bitwidth configurations are adopted for every base model due to compatibility constraints and computational limitations. In total, our evaluation encompasses 63 distinct model configurations that we evaluate in the reliability assessment framework. As we only report the best-performing model for each bit width in Section 4, both QuaRot and Quanto are not included in the scaling laws figures as they do not outperform other quantization techniques. In addition, we note that we use AQLM-PV for the 2-bit quantization, which corresponds to AQLM quantization with an additional PV tuning step. AQLM-PV provides increased performance improvement compared to AQLM. We run $63 * 3 * (1 + 15 * 2) = 5859$ experiments in total, where 63 is the number of models, 3 is the number of the QA datasets, 15 is the number of evaluations, and 2 corresponds to the two perturbation intensities 4 and 16.

For the quantization using Bitsandbytes (Dettmers et al., 2022), HQQ (Badri & Shaji, 2023), Quanto (Team, 2023) and GPTQ (3-bit), we use the Hugging Face Transformers (Wolf et al., 2019) default implementation, licensed under the Apache-2.0 license. GPTQ is licensed under the Apache-2.0 license, while AWQ is licensed under the MIT license. All AQLM, QuaRot, and QoQ models are loaded directly from HuggingFace, licensed under the Apache License 2.0. The LLaMA-3 and LLaMA-3.2 model families we used in our experiments are licensed under the Llama 3 Community License Agreement.

Table 1: Quantization techniques used in our reliability evaluation framework. ✓ corresponds to models included in the reliability assessment, and × corresponds to quantization-precision combinations we do not include.

Quantization Method		Model Size			
Method	Bit	1B	3B	8B	70B
Base	16-bit	✓	✓	✓	✓
AQLM	2-bit	×	×	✓	×
AQLM-PV	2-bit	✓	✓	✓	×
AWQ	4-bit	✓	✓	✓	✓
BNB	8-bit	✓	✓	✓	✓
	4-bit	✓	✓	✓	✓
GPTQ	8-bit	✓	✓	✓	×
	4-bit	✓	✓	✓	×
	3-bit	✓	✓	✓	×
	2-bit	✓	✓	✓	×
HQQ	8-bit	✓	✓	✓	✓
	4-bit	✓	✓	✓	✓
	3-bit	✓	✓	✓	✓
	2-bit	✓	✓	✓	✓
QoQ	4-bit	×	×	✓	×
Quanto	8-bit	✓	✓	✓	✓
	4-bit	✓	✓	✓	✓
	2-bit	✓	✓	✓	✓
QuaRot	8-bit	×	×	✓	×
	4-bit	×	×	✓	×

Table 2: Summary of the evaluated benchmarks. We provide the corresponding bit-level inference scalings in Section 4 and Section D.

Task & Ability	Benchmark
Language Modeling	PTB (Marcus et al., 1993)
	C4 (Raffel et al., 2020)
	WikiText2 (Merity et al., 2016)
Open-Ended QA Generation for General Knowledge & Dialog	TriviaQA (Joshi et al., 2017)
	CoQA (Reddy et al., 2019)
In-Context Learning	MMLU (Hendrycks et al., 2020)
	CEval (Huang et al., 2023)
Instruction Following	HellaSwag (Zellers et al., 2019)
	ARC (Clark et al., 2018)
Reasoning	PIQA (Bisk et al., 2020)
	CommonsenseQA (Talmor et al., 2018)
Understanding	RACE (Lai et al., 2017)

A.2 EVALUATION DATASETS AND GENERATION

For the evaluation, we use two widely-used datasets for assessing the reliability of LLMs, TriviaQA (Joshi et al., 2017) and CoQA (Reddy et al., 2019). TriviaQA consists of 95,000 question-answer pairs to assess reading comprehension capabilities, while CoQA consists of 8,000 question-answer pairs. We further evaluate on the multiple-choice question answering CommonsenseQA (Lin & Och, 2004) dataset. We also evaluate on additional widely used benchmarks such as HellaSwag (Zellers et al., 2019), MMLU (Hendrycks et al., 2020), and Arc-Easy (Clark et al., 2018). We summarize all evaluation benchmarks in Table 2. For all datasets, we limit the evaluation to 1000 uniformly sampled prompts, due to the increased number of evaluation combinations as we consider four base models, eight quantization models, and five different bit precision levels. We randomly sample 1000 samples from the datasets for 5 random seeds, and evaluate the accuracy. We compare the accuracies over the sampled sets with the accuracy averaged across the entire datasets. We show in Fig. 9 that the accuracy on the subsets is close to the full dataset evaluation. During generation, we limit the generated sequence length to 20 tokens per input prompt. During the generation, we use multinomial sampling with a temperature parameter of 0.7.

We conduct our experiments using GTX 1080 Ti (11GB) and A100 (40GB) GPUs. For smaller models, specifically all 1B and 3B models (excluding AQLM and GPTQ variants), we use a single GTX 1080 Ti GPU. Medium-sized models, including the 1B and 3B AQLM variants, GPTQ, the 8-bit versions, and all 8B models, are evaluated on a single A100 GPU. For the largest 70B models, we use five A100 GPUs in parallel to handle loading and evaluation efficiently. For the evaluation runtime given a single perturbation (or no perturbation), the average evaluation time is approximately 5 minutes on the GTX 1080 Ti for the small models, and 4 minutes on the A100, and roughly 24 minutes for the 70B models on the five A100 GPUs.

B ADDITIONAL DETAILS ON THE PERTURBATIONS

In addition to the character-level and word-level perturbations described in Section 3.2, we provide additional details on additional perturbations in the following:

- Deletion: For character-level perturbation, we randomly remove characters from the sentence; at the word level, we remove words from text, primarily targeting filler words (e.g., "and", "to", "also", "actually") to preserve the important part of the prompt (Moradi & Samwald, 2021). We use 508 filler words in total.
- Leetspeak: Substitutes characters with visually similar numerals or symbols (like replacing 'e' with '3'). We provide additional examples in Table 3. We use 93 Leetspeak examples.

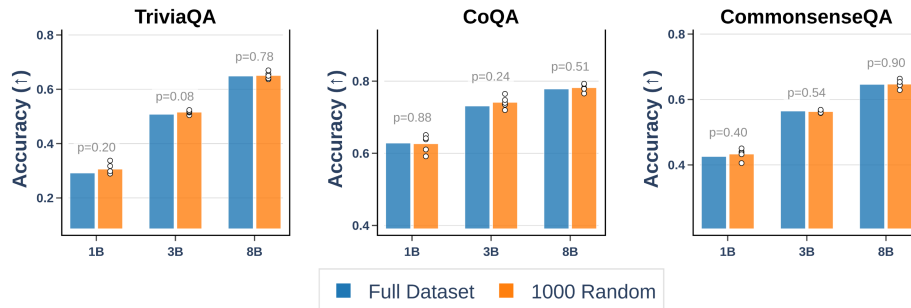


Figure 9: Comparison of the accuracy when evaluating on the full datasets versus evaluating on 1000 randomly sampled prompts (averaged over 5 random seeds).

Table 3: Examples of leetspeak character perturbations.

Leetspeak Character Substitutions			
A → @	a → @	B → 8	b → 6
C → (c → ©	D →)	d → δ
E → 3	e → €	G → 6	g → 9
H → #	I → 1	i → !	J → 7
K → <	L → £	l →	O → 0
o → °	P → ?	R → ®	S → 5
s → §	T → 7	w → ω	X → ×

- **Noise:** Inserts punctuation or digits as noise characters distributed randomly throughout the text, using a configurable noise character set.
- **Replacement:** Substitutes characters with adjacent keyboard alternatives to simulate realistic typos, using a keyboard layout mapping maintaining case sensitivity (Ackerman et al., 2024).
- **Swapping:** Exchanges adjacent characters to simulate typographical errors; at the word level, exchanges adjacent words while preserving punctuation and maintaining the question-answer prompt structure (Moradi & Samwald, 2021; Wang et al., 2024).
- **Repetition:** Duplicates characters at random positions; at the word level, duplicates words while handling punctuation preservation and maintaining overall text structure (Moradi & Samwald, 2021).
- **Case Change:** Alters letter case patterns, toggling between uppercase and lowercase only for alphabetic characters (Moradi & Samwald, 2021).
- **Emoji:** A novel perturbation type that inserts emoji characters within text, distributing them across words using a configurable emoji set. We use 115 emoji characters in total.
- **Slang:** Inserts internet slang expressions (like "lol", "rofl", "imo") using a predefined dictionary of common terms, distributing insertions randomly throughout the text.
- **Translation:** Translates words and phrases through Google Translate API across seven languages (Spanish, French, German, Italian, Russian, Chinese, Japanese). As opposed to the semantic-level translation perturbation introduced in Zhu et al. (2024), our method does not translate phrases back to English, simulating multi-lingual user outputs.
- **Insertion:** Randomly inserts characters between existing characters at the character level; at the word level, adds contextually relevant words using RoBERTa masked language model to predict insertions while preserving text coherence. This approach is methodologically similar to the synonym insertion implemented by Moradi & Samwald (2021), but only adds words and does not change them.

Table 4: We report the total model bits (in GB), the inference memory (in GB), the per-token latency (ms), corresponding to the time spent to generate each token in the output, and the number of decoded tokens per second. We evaluate on a single A100 GPU.

Model	Bitwidth	Total Model Bits (GB)	Inference Memory (GB)	Per-Token Latency (ms)	Decoded tokens per second
Qwen3-4B	16-bit	8.217	8.409	4.103	266.35
Qwen3-4B	8-bit	4.108	4.300	2.510	462.66
Qwen3-8B	16-bit	15.256	15.476	9.884	110.30
Qwen3-8B	8-bit	7.628	7.848	5.806	200.50
Qwen3-8B	4-bit	3.814	4.034	3.766	339.16
Qwen3-32B	4-bit	15.250	15.478	8.719	150.29

For the leetspeak character perturbations, we provide examples in Table 3. Each perturbation is applied at varying intensity levels of 4 and 16 to systematically evaluate model robustness across multiple intensities. We note that for the word perturbations presented in Fig. 2, the number of perturbed words in the input prompt corresponds to the minimum between the perturbation intensity and the length of the input prompt.

C ADDITIONAL EFFICIENCY METRICS

In this section, we examine how the total model bits metric relates to several commonly used efficiency measures, including inference memory, latency, and throughput. A quantitative comparison of these metrics is provided in Table 4 for different models from the Qwen3 model family. As introduced in Section 3.3, the total number of bits B is defined as the product of the number of model parameters and their weight precision (in bits). This quantity corresponds directly to the model’s storage memory. The total model bits further maps to the inference memory, measured as:

$$\text{Inference memory} = P \times \text{Avg-Bitwidth} + \text{Overhead}, \quad (7)$$

where P is the total number of parameters, and the Overhead term accounts for the additional memory used during inference (e.g., KV cache, activation). In practice, the overhead is generally negligible relative to the storage memory, which implies that inference memory scales almost linearly with the total model bits.

For inference latency, the relationship with total model bits is less direct but still significant. The overall latency is determined by two phases: (1) the pre-fill phase and (2) the decode phase. During prefill, the model processes the input sequence and constructs the key–value (KV) cache. This stage is typically compute-intensive and can fully utilize GPU compute units. During the decode phase, the model generates output tokens sequentially. Each token is predicted based on the previously generated tokens and the information stored in the KV cache from the prefill stage. Lower-precision numbers can improve speed because they reduce the amount of data that needs to be moved in memory and allow computations to be executed more quickly. For instance, on modern GPUs such as H100, 8-bit operations can achieve significantly higher FLOPS than 32-bit operations. However, this improvement also depends on specialized hardware support¹. For future work, it would be interesting to investigate scaling laws as a function of latency, as it depends not only on the model, but also on the hardware. We note that we use a batch size of 1 in our setup (see Section A.1) and compute the corresponding token latency and throughput.

The throughput defines the number of output tokens that can be predicted per time unit. For sequential, non-parallel decoding, such as autoregressive LLM, latency and throughput are directly coupled. More specifically, for a batch size of 1, the throughput corresponds to $\frac{1}{\text{Latency}}$. Since decoding is inherently sequential and the setup is compute-bound, improving the latency directly improves throughput.

In Table 4, we compare the different efficiency metrics for models from the Qwen3 model family. Specifically, we select models with 4B, 8B, and 16B parameters. For the quantization, we use BitsandBytes (Dettmers et al., 2022) and quantize the full-precision models to 4 and 8 bits.

¹<https://resources.nvidia.com/en-us-gpu-resources/h100-datasheet-24306>

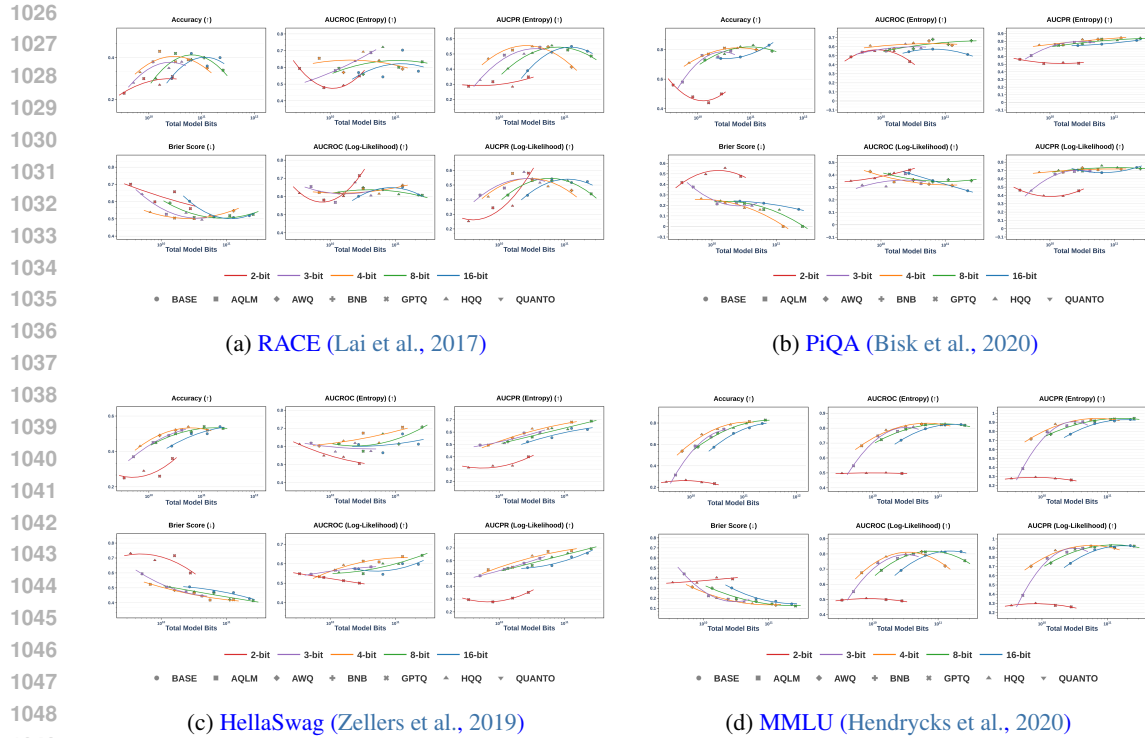


Figure 10: Bit-level scaling trends of Qwen3 models across four benchmarks.

D RELIABILITY SCALING TRENDS ACROSS DIFFERENT BENCHMARKS

Reliability scaling trends of Qwen3 models We evaluate four base models from the Qwen3 model family, with sizes of 4B, 8B, 14B, and 32B, and their corresponding quantized models using 6 different PTQ methods. We provide results in Fig. 10. We evaluate the reasoning abilities on the PiQA benchmark in Fig. 10b, and the understanding abilities on RACE in Fig. 10a. For instruction-following assessment, we use the HellaSwag benchmark and provide results in Fig. 11b. For in-context learning, we evaluate on the widely-used MMLU dataset in Fig. 10d. Across different datasets, model sizes, and bitwidths, we observe a sweet spot at 4-bit quantization. Both GPTQ and HQQ provide the best performance for 4-bit quantization. We further note that for Qwen3 models, 3-bit quantization can provide favorable performance in terms of zero-shot performance and reliability.

Reliability scaling trends of LLaMA-3 models In addition to the performance and reliability bit-level inference scalings provided in Section 4, we extend the evaluation to in-context learning and instruction-following tasks to assess the emergent abilities of quantized LLMs from the LLaMA-3 model family. For in-context learning, we provide the bit-level inference scaling plots under Fig. 11a for the MMLU task. For instruction-following, we evaluate on HellaSwag in Fig. 11b and ARC in Fig. 11c. We further assess the open-ended generation on CoQA in Fig. 11d, which is a conversational question-answering task that tests the dialog understanding capabilities of models. Additional bit-level scalings on the instruction-tuned LLaMA models are presented in Fig. 12. For the 2-bit precision, AQLM-PV provides the best zero-shot accuracy. For 3-bit models, HQQ outperforms GPTQ across different metrics. For 4-bit models, both AWQ (Lin et al., 2024a) and GPTQ (Frantar et al., 2022) generally provide the best downstream task performance and reliability.

1080
1081
1082
1083
1084
1085
1086
1087
1088
1089
1090
1091
1092
1093
1094
1095
1096
1097
1098
1099
1100
1101
1102
1103
1104
1105
1106
1107
1108
1109
1110
1111
1112
1113
1114
1115
1116
1117
1118
1119
1120
1121
1122
1123
1124
1125
1126
1127
1128
1129
1130
1131
1132
1133

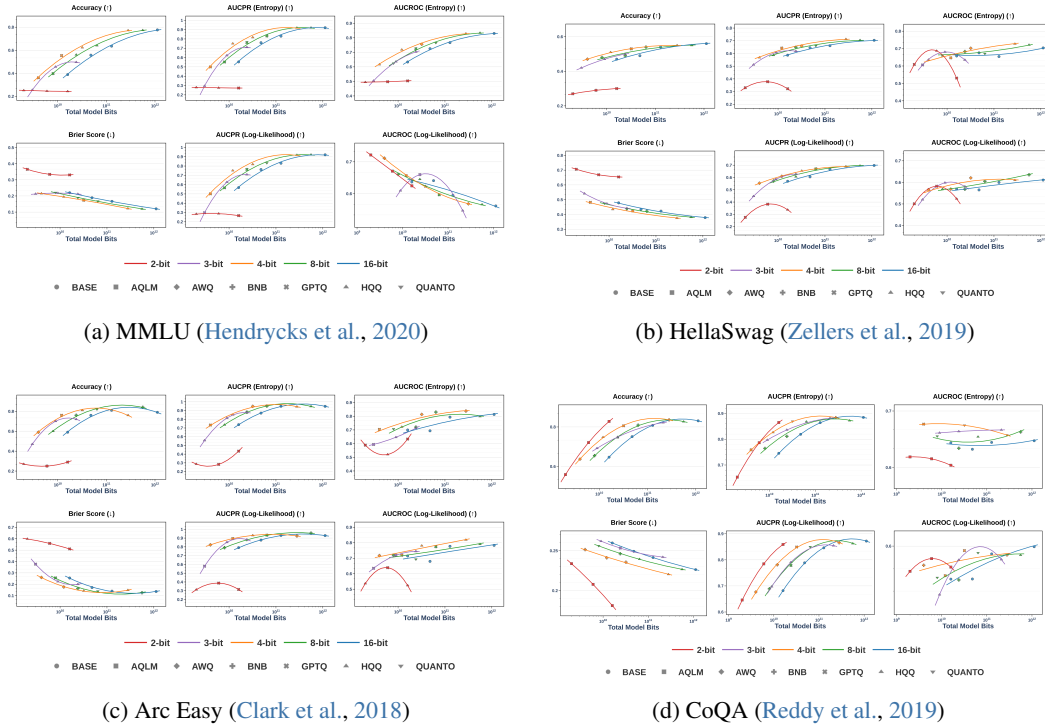


Figure 11: Bit-level scaling trends of LLaMA models across four benchmarks.

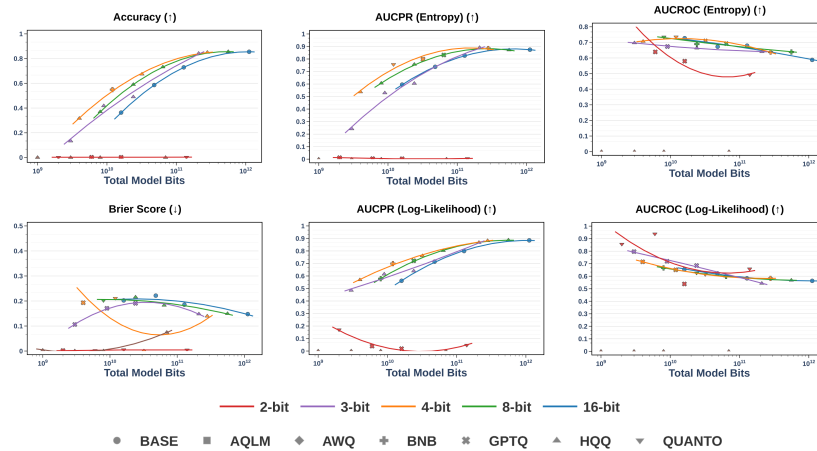


Figure 12: Scaling behavior of the reliability metrics of the **instruction-tuned** LLaMA models on **TriviaQA**.

Table 5: Performance across different perturbation intensities on the TriviaQA dataset

Model	Intensity	Metrics		
		Accuracy	AUCROC (Entropy)	AUCPR (Entropy)
LLaMA-3.2-1B	0	0.338 ± 0.000	0.683 ± 0.000	0.518 ± 0.000
	4	0.192 ± 0.050	0.636 ± 0.029	0.264 ± 0.084
	16	0.078 ± 0.077	0.578 ± 0.069	0.098 ± 0.118
LLaMA-3.2-3B	0	0.549 ± 0.000	0.722 ± 0.000	0.746 ± 0.000
	4	0.384 ± 0.064	0.689 ± 0.020	0.534 ± 0.083
	16	0.189 ± 0.126	0.608 ± 0.076	0.234 ± 0.170
LLaMA-3-8B	0	0.691 ± 0.000	0.715 ± 0.000	0.847 ± 0.000
	4	0.519 ± 0.069	0.691 ± 0.022	0.687 ± 0.065
	16	0.283 ± 0.156	0.640 ± 0.051	0.357 ± 0.189
LLaMA-3-70B	0	0.728 ± 0.000	0.503 ± 0.000	0.729 ± 0.000
	4	0.706 ± 0.037	0.557 ± 0.036	0.736 ± 0.036
	16	0.503 ± 0.145	0.595 ± 0.063	0.544 ± 0.136

Table 6: [Recommendation](#) list of the best quantization methods per model size and bit width across different evaluation metrics on the unperturbed TriviaQA dataset.

Base Model	Bit Width	Accuracy	AUCROC (Entropy)	AUCPR (Entropy)	AUCPR (Log-Lik.)
1B	2	AQLM	AQLM	AQLM	AQLM
1B	4	AWQ	GPTQ	AWQ	GPTQ
1B	8	GPTQ	Quanto	GPTQ	BNB
3B	2	AQLM	AQLM	AQLM	AQLM
3B	3	HQQ	HQQ	HQQ	HQQ
3B	4	HQQ	GPTQ	HQQ	GPTQ
3B	8	Quanto	BNB	Quanto	Quanto
8B	2	AQLM	AQLM	AQLM	AQLM
8B	3	HQQ	HQQ	HQQ	HQQ
8B	4	HQQ	GPTQ	AWQ	HQQ
8B	8	HQQ	Quanto	HQQ	GPTQ
70B	3	HQQ	HQQ	HQQ	HQQ
70B	4	AWQ	AWQ	AWQ	AWQ
70B	8	HQQ	BNB	Quanto	HQQ

E RELIABILITY SCALING TRENDS ON PERTURBED BENCHMARKS

In this section, we provide additional results to show the scaling behavior of the accuracy, the quality of the uncertainty estimates, the log-likelihood, and the calibration using the perturbed prompts. In particular, we provide the results for the Word Slang perturbation in Fig. 13 and the Leetspeak perturbation in Fig. 14. For all experiments, we fit a log-quadratic function per bit width, and only show the best-performing model for every bit level. We further report the mean and standard deviation of the accuracy and the reliability metrics of the four base LLaMA-3 models, under unperturbed and perturbed input prompts, in Table 5. Additionally, in Table 7, we provide a list of the best quantization methods per base model and precision for two different perturbation intensities. For the 2-bit precision, AQLM-PV provides the best performance on the perturbed datasets. For 3-bit models, HQQ outperforms GPTQ across different metrics. For 4-bit models, HQQ (Badri & Shaji, 2023) and GPTQ (Frantar et al., 2022) generally provide the best downstream performance and reliability under perturbation, followed by AWQ (Lin et al., 2024a).

1188
1189
1190
1191
1192
1193
1194
1195
1196
1197
1198
1199
1200
1201
1202
1203
1204
1205
1206
1207
1208
1209
1210
1211
1212
1213
1214
1215
1216
1217
1218
1219
1220
1221
1222
1223
1224
1225
1226
1227
1228
1229
1230
1231
1232
1233
1234
1235
1236
1237
1238
1239
1240
1241

Table 7: [Recommendation](#) list of the best quantization methods per model size and bit width across different evaluation metrics on the **perturbed** TriviaQA dataset. We average the performance over all 15 perturbations with an intensity equal to 4.

Base Model	Bit Width	Accuracy	AUCROC (Entropy)	AUCPR (Entropy)	AUCPR (Log-Lik.)
1B	2	AQLM	AQLM	AQLM	-
1B	4	AWQ	GPTQ	AWQ	HQQ
1B	8	HQQ	GPTQ	HQQ	BNB
3B	2	AQLM	AQLM	AQLM	-
3B	3	HQQ	HQQ	HQQ	HQQ
3B	4	HQQ	GPTQ	HQQ	Quanto
3B	8	Quanto	BNB	Quanto	HQQ
8B	2	AQLM	AQLM	AQLM	-
8B	3	HQQ	HQQ	HQQ	HQQ
8B	4	AWQ	GPTQ	AWQ	HQQ
8B	8	HQQ	Quanto	GPTQ	Quanto
70B	3	HQQ	HQQ	HQQ	HQQ
70B	4	AWQ	AWQ	AWQ	HQQ
70B	8	HQQ	BNB	HQQ	HQQ

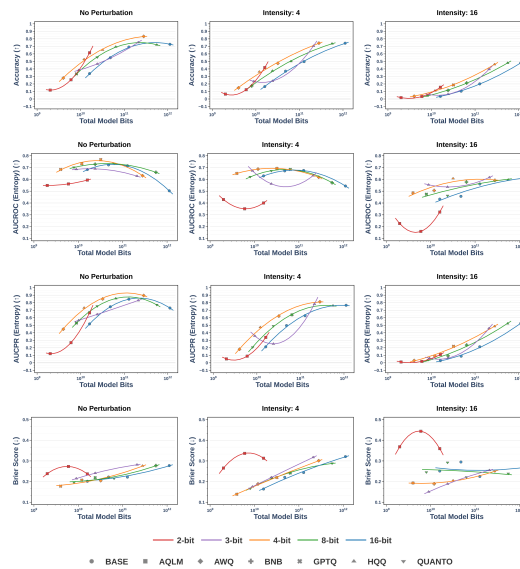


Figure 13: Scaling behavior of the accuracy and various uncertainty quantification and calibration metrics on the unperturbed TriviaQA dataset, as well as the perturbed prompts using the **word slang** perturbation using two perturbation intensities of 4 and 16.

1242
1243
1244
1245
1246
1247
1248
1249
1250
1251
1252
1253
1254
1255
1256
1257
1258
1259
1260
1261
1262
1263
1264
1265
1266
1267
1268
1269
1270
1271
1272
1273
1274
1275
1276
1277
1278
1279
1280
1281
1282
1283
1284
1285
1286
1287
1288
1289
1290
1291
1292
1293
1294
1295

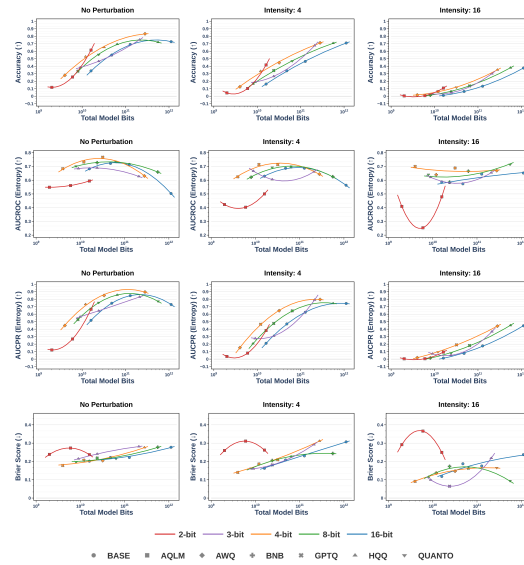


Figure 14: Scaling behavior of the accuracy and various uncertainty quantification and calibration metrics on the unperturbed TriviaQA dataset, as well as the perturbed prompts using the **Leetspeak** perturbation using two perturbation intensities of 4 and 16.

F ADDITIONAL ABLATIONS

In this section, we provide additional ablations across temperature used for sampling and the length of the generated sequences. We note that we limit the evaluation to 100 samples from the TriviaQA dataset. We first examine the bit-level inference scalings under different decoding strategies. Specifically, evaluate the open-ended generation of base and quantized LLMs on TriviaQA, where we sample with various temperature values in 0.2, 0.7, 1.0. We present the qualitative results in Fig. 15. Overall, the performance and reliability metrics exhibit consistent trends across temperature settings. In particular, accuracy increases with the total number of model bits, with 4-bit models achieving the strongest performance. For reliability, we observe a pronounced peak for 4-bit quantized models. However, as the temperature increases to 0.7 and 1.0, 3-bit quantized models yield the best Brier scores, given a fixed total model bits. In Fig. 3, we truncate the generation of models to 20 tokens. We explore longer generations using an increased number of tokens. We present results in Fig. 16.

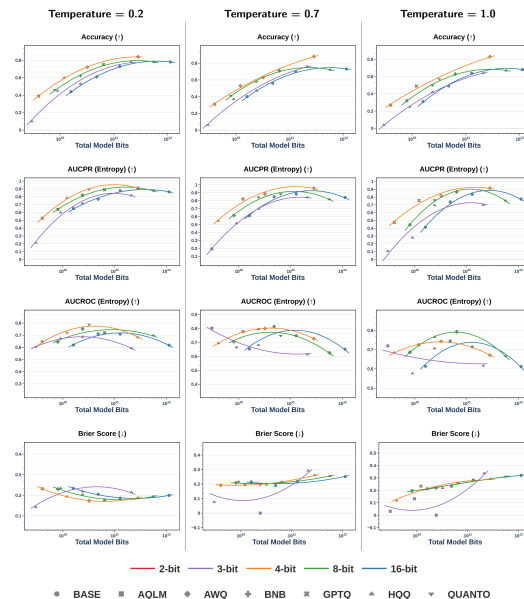


Figure 15: Bit-level inference scaling trends on TriviaQA for various temperature values for sampling.

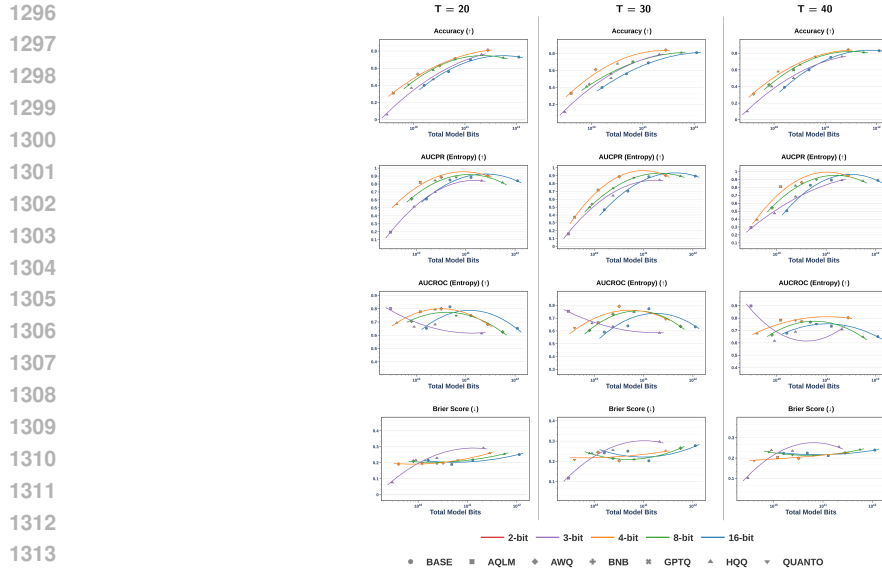


Figure 16: Bit-level inference scaling trends on TriviaQA for different numbers of output tokens.

G WHY DOES 4-BIT QUANTIZATION OFFER A FAVORABLE PERFORMANCE?

The goal of model quantization is to create a more efficient model from a full-precision base model, while maintaining as close a distance to its full-precision counterpart. While both perplexity and accuracy metrics are essential for evaluating the generalization capabilities of quantized models, they fail to capture the shifts in model behavior that can occur post-compression. To quantify this behavioral shift, we measure the Kullback-Leibler Divergence (KLD) between the token distributions predicted by the base model, $P_{\theta_B}(\mathbf{x}_t | \mathbf{x}_{<t})$, and those predicted by the compressed model, $P_{\theta_C}(\mathbf{x}_t | \mathbf{x}_{<t})$ as follows:

$$\frac{1}{|\mathcal{D}_{\text{test}}|} \sum_{\mathbf{x} \in \mathcal{D}_{\text{test}}} \frac{1}{T} \sum_{t=1}^T \text{KLD}(P_{\theta_B}(\mathbf{x}_t | \mathbf{x}_{<t}) \| P_{\theta_C}(\mathbf{x}_t | \mathbf{x}_{<t})), \quad (8)$$

where $\mathbf{x} = (\mathbf{x}_1, \dots, \mathbf{x}_T) \sim \mathcal{D}_{\text{test}}$ is a sequence sampled from a test dataset, and T defines the number of tokens in the sequence. In Fig. 17, we provide the bit-level scaling trends of the KL-Divergence measured between the token distributions of base and quantized models. We consider 3 LLaMA models with 1B, 3B, and 8B parameters, and quantize them to different bitwidths. First, we observe that 2-bit quantized models exhibit a substantial behavioral shift relative to their full-precision counterparts, which likely contributes to their consistently poor performance. For 3-bit quantization, the KL divergence remains noticeably larger than that of 4-bit models. However, as model size increases from 1B to 8B parameters, the behavioral shift induced by 3-bit quantization diminishes. This reduction helps explain the improved downstream performance of larger 3-bit models (see Fig. 4). In contrast, 4-bit quantization maintains a small KL divergence across different model scales. We hypothesize that this limited behavioral shift allows 4-bit models to retain strong generalization capabilities while still achieving a substantial reduction in total model bits.

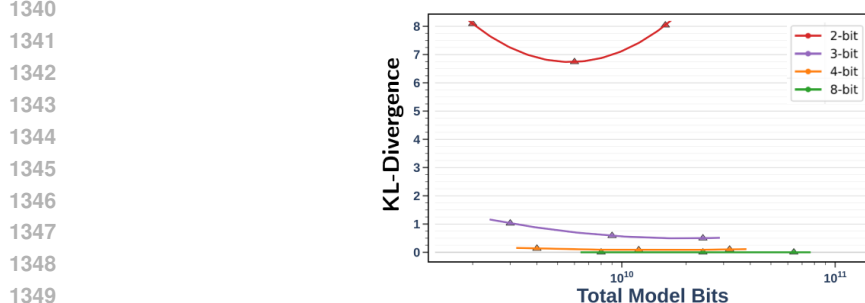


Figure 17: Scaling trends of the KL-Divergence between base models and quantized counterparts on WikiText.

H HOW DOES QUANTIZATION-AWARE TRAINING AFFECT THE SCALING TRENDS?

While our study primarily focuses on state-of-the-art post-training quantization techniques for LLMs, we investigate in the following how quantization-aware training (QAT) influences the performance and reliability scaling trends. QAT is especially compelling for extreme quantization regimes, as post-training quantizations often result in substantial performance degradation, as shown in Fig. 5.

In the following, we examine the recent EfficientQAT (Chen et al., 2025b) method, which consists of two stages: block-wise training of all model parameters followed by end-to-end training of the quantization parameters. We apply QAT to three LLaMA-3 models with 7B, 13B, and 70B parameters and evaluate 4-bit and 2-bit quantized models as well as their full-precision counterparts. We present qualitative results of the bit-level inference scalings in Fig. 18. We find that 4-bit quantized models generally offer favorable zero-shot performance and reliability for a fixed total bit budget. EfficientQAT (Chen et al., 2025b) achieves impressive results in 2-bit scenarios, improving the zero-shot performance and reliability scaling trends compared to PTQ approaches. However, a performance gap remains compared to higher bitwidths.

We limit the evaluation to the EfficientQAT approach due to time and resource constraints. Extending the bit-level reliability scaling study to different QAT approaches (Liu et al., 2024; Ma et al., 2024; Xu et al., 2024a) and performing a more thorough comparison across different model backbones, tasks, and bit precisions could yield novel insights, which we leave for future work. While QAT techniques are promising for extremely low bit-widths, there remains a need for more efficient and practical approaches. For example, while BitNet b1.58 (Ma et al., 2024) achieves nearly lossless ternary quantization, it requires retraining LLMs from scratch on the entire pre-trained dataset. This makes it impractical for huge models and restricts its validation to 3B models trained on 100B tokens, limiting its applicability for comprehensive scaling law studies across varying model sizes.

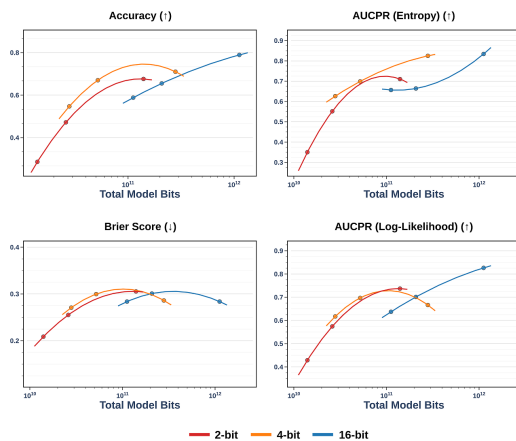


Figure 18: Bit-level inference scaling trends of quantized LLaMA models using EfficientQAT (Chen et al., 2025b).